Predicting the site-specific distribution of agrochemical spray deposition in vineyards at multiple phenological stages using 2D LiDAR-based primary canopy attributes

Anice Cheraiet, Olivier Naud, Mathilde Carra, Sébastien Codis, F. Lebeau,
James Taylor

HAL Id: hal-03339890

https://hal.inrae.fr/hal-03339890

Submitted on 10 Nov 2023

1   **Predicting the site-specific distribution of agrochemical spray deposition in vineyards at**

2   **multiple phenological stages using 2D LiDAR-based primary canopy attributes**

3

4   A. Cheraiet[a,b,*], O. Naud[a], M. Carra[a], S. Codis[b], F. Lebeau[a,c] and J. Taylor[a].

5   [a] ITAP, Univ Montpellier, INRAE, Institut Agro, Montpellier, France

6   [b]IFV French Vine and Wine Institute, 3430 Route de l'Espiguette, Le Grau-du-Roi, France

7   [c]Biosystems Dynamics and Exchanges (BioDynE), TERRA Teaching and Research Center, Gembloux

8   Agro-Bio Tech, University of Liege, Gembloux, Belgium

9   *Correspondence: anice.cheraiet@vignevin.com

10

11   **Abstract**

12

13   Predicting the dose to be applied on the basis of the structural characteristics of the plant canopy is a

14   crucial step for the optimization of the spraying process. Mobile 2D LiDAR sensor data and local

15   measurements of deposition rates from a face-to-face sprayer were made across eight fields in two

16   Mediterranean vineyards at four dates in 2016 and 2017. Primary canopy attributes (height, width and

17   density) were calculated from the LiDAR sensor data and the leaf wall area (LWA) determined.

18   Multivariate models to predict the deposition distribution, as deciles, as a function of the primary

19   canopy attributes were constructed and calibrated using the 2017 data and validated against the 2016

20   data. The prediction quality and uncertainty of these multivariate statistical models at various stages of

21   growth was evaluated by comparison with a previously proposed univariate deposition models based

22   on LWA at the same growth stages. The results showed that multivariate models can predict the

23   distribution of deposits from a typical face-to-face sprayer more accurately ($0.76 < R^2 < 0.94$), and

24   robustly ($10\% < nRMSEp < 24\%$) than LWA-based univariate prediction models over the whole

25   growing season. This improvement was especially clear for the lowest deciles (D1 to D5) of the

26   deposition distribution. Results also demonstrated the importance of canopy density to provide

27   relevant and complementary information to canopy dimensions when predicting deposition deciles

28   with the multivariate models. The improved ability of multivariate models to predict underestimated

29   deposition ($-1.5\% < bias < -3.2\%$) when compared to univariate models makes it possible to consider a

30 reduction in the plant protection products while guaranteeing a safety margin for winegrowers when

31 spraying. These predictive multivariate models could enable variable-rate sprayers to modulate doses

32 at an intra-plot scale, which would allow a potential reduction in the quantities of plant protection

33 products to be applied.

34

35 **Keywords:** Canopy density; Variable-rate spraying; 3D vine; Leaf Wall Area; Log-linear models

36

37   **1. Introduction**

38

39 The current regulatory context, and the very high societal demand for a reduction in the use of

40 pesticides in viticulture, has led to a reconsideration of the entire plant protection process (EPPO,

41 2016). Achieving the objective of reducing pesticides will require the implementation of different and

42 complementary approaches, including biological control (Flint and van den Bosch, 1982), the

43 selection of resistant varieties (Vivier and Pretorius, 2002), optimization of spraying technologies

44 (Llorens et al., 2011a) and adjustment of plant protection product (PPP) doses according to vegetation

45 architecture (Walklate et al., 2011). Dose adjustment based on varying canopy size and shape, has

46 been widely discussed in previous research (Gil et al., 2019), and seems especially important in

47 countries, like France, where the registered dose rates of PPPs are still based on a fixed value per

48 hectare (Codis, 2016) and calculated independently of the quantity of vegetation to be treated. There

49 are two interrelated issues concerning dose reasoning. The first is dose expression. Some authors

50 believe that a new dose expression that explicitly takes into account canopy development, which will

51 be mostly influenced by growth stages, training systems and varietal characteristics, would be an

52 important step toward a more efficient use of PPPs (Solanelles et al., 2006). The second issue is to

53 define and select the most suitable crop parameters to be used for locally adjusting dose rates to

54 canopy architecture (Walklate et al., 2011).

55

56 Historically, simple manual measurements of primary canopy attributes, such as height, width and the

57 distance between rows, have been used to generate integrative indicators of canopy geometry, such as

58 the leaf wall area (LWA) (Koch, 1993) or tree row volume (TRV) (Byers et al., 1971). These

59 integrative indicators have become widely used as they provide a simple expression of the complex

60 architecture of the vegetation for modelling the PPP dose to be applied (Walklate and Cross, 2012). In

61 particular, the LWA has been identified as a good compromise between accuracy and simplicity to

62 establish a linear relationship between canopy geometry and the recommended amount of PPP

63 (Walklate and Cross, 2012) and it is now used to standardise PPP trials. However, the derivation of

64 these integrative indicators has two disadvantages: (i) they are too simplistic to properly model foliar

65 deposition (Cheraiet et al., 2019) under variable production conditions as the same LWA or TRV

66 value may reflect very different vegetation characteristics and PPP needs; and (ii) they are typically

67 based on measurements at only a few points within a vineyard with an assumption of a homogeneous

68 canopy structure over the entire area. When sampling is scarce, then local, site-specific variations in

69 canopy geometry cannot be taken into account when applying PPP.

70

71 To address the limitation in the spatial resolution of manual measurements, different high-resolution

72 spatial sensing systems have been proposed in recent years (Rosell and Sanz, 2012). Among these,

73 LiDAR systems have been reported to be effective for site-specific measurements of canopy size and

74 shape (Colaço et al., 2018). LiDAR sensors make it possible to obtain digitalised 3D point clouds,

75 from which a large amount of plant architecture information, such as canopy height, width (Rosell et

76 al., 2009;) and density (Walklate et al., 2002; Llorens et al., 2011b) can be obtained with a high level

77 of accuracy and repeatability (Moorthy et al., 2011). Due to the high spatial resolution of these LiDAR

78 data, these attributes can be calculated at any scale, from individual vines to entire vineyards.

79

80 Obtaining primary canopy dimensions from sensors, including LiDAR sensors, enables the calculation

81 of integrative indicators, such as the TRV or LWA, at high spatial resolutions. So far, this ability has

82 been used to build univariate empirical models to predict the mean foliar pesticide deposition (Llorens

83 et al., 2010), typically using power or logarithmic regression models (Siegfried et al., 2007; Bastianelli

84 et al., 2017). Bastianelli et al. (2017) highlighted the ability of these univariate empirical models to

85 discriminate between different types of spraying equipment and noted that the prediction quality for a

86   side-by-side sprayer using a univariate empirical based on LWA was sufficient to be considered for

87   production applications.

88

89   However, empirical models that are based on a unique integrative indicator do have limitations,

90   particularly when the objective is to adjust dose rates under a wide variety of vineyard conditions and

91   training systems (Llorens et al., 2010). Vine management and pruning is normally standardised within

92   blocks, which results in a strong correlation between canopy height and width. However, across

93   different blocks, vineyards and regions, the relationship between primary canopy attributes differs

94   according to local trellising systems, management strategies and vine varieties. Cheraiet et al. (2019)

95   demonstrated that the prediction uncertainty of univariate empirical models varied greatly between

96   vineyards in southern France, especially in the early stages of vegetation development when correct

97   PPP is needed for effective crop protection. Moreover, univariate empirical models have only been

98   used to predict the mean deposition, and not the distribution of deposition within the canopy. The

99   distribution of deposition within the canopy will be dependent on both the characteristics of the

100   canopy (Palleja and Landers, 2015) and the characteristics of the sprayer (type and settings: nozzle

101   type, size and pressure, air velocity and airflow direction) (Derksen et al., 2007).

102

103   Therefore, whilst integrative indicators have proved useful for the industry when used with low-

104   resolution measurements, their suitability for the development of precision spraying approaches using

105   high-resolution information from sensing systems is questionable, especially when knowledge of

106   deposition distribution rather than mean deposition is desirable. Sensor systems are now capable of

107   generating high-resolution spatial and temporal information on primary canopy attributes, including

108   height, width and some indication of density. However, so far, canopy density information has not

109   been well incorporated into deposition prediction models within a vegetation canopy, even though the

110   literature highlights the importance of this attribute (Pergher and Petris, 2008). It follows that

111   multivariate statistical modelling approaches to predict the distribution of deposits at different stages

112   of canopy development that are based on primary canopy attributes should be investigated, and are

4

113   hypothesised to be better than previously used univariate modelling approaches based on an

114   integrative indicator of canopy architecture.

115

116   In order to test this hypothesis and to facilitate the optimization of spraying efficiency, the research

117   presented here aims to investigate the use of multivariate statistical models to predict the distribution

118   of deposits based on primary canopy attributes (dimensions, density) derived from a LiDAR sensing

119   system. The specific objectives are to:

120   (1) Propose a primary canopy density attribute, based on 2D LiDAR data, that can be included in the

121   modelling;

122   (2) Construct, calibrate and validate multivariate models, based on primary canopy attributes, to

123   predict the distribution of intercepted deposits in vineyard canopies applied by a side-by-side sprayer

124   at multiple growth stages over the growing season;

125   (3) Assess the prediction quality and uncertainty of these multivariate models relative to a previously

126   proposed univariate model that is based on an integrated indicator of canopy size (LWA).

127

128   **2.   Materials and Methods**

129

130   *2.1. Fields trials*

131

132   Two vine estates with blocks of different varieties and contrasting vigour were chosen for the study in

133   2016 and 2017. The 2016 trials were at the Mas Piquet Estate in Grabels, close to Montpellier,

134   Hérault, France, and the 2017 trials at the Domaine Chapitre Estate in Villeneuve les Maguelone,

135   Hérault, France. The training system, vine vigour and grape varieties in the two estates are

136   characteristic of vineyards in southern France. Vines were trellised in 2.5m rows with a 1.0m vine

137   spacing within rows using a cordon Royat or Guyot system that comprised a cordon wire and at least

138   one trellising wire.

139

In 2016, spray deposition measurements and 2D LiDAR sensor canopy characterization was performed on four plots with four different varieties, while in 2017, measurements were performed on five plots with five different varieties. In both years there were 4 surveys (dates of measurements) that generated a range of growth stages (BBCH scale, Lorenz et al., 1994) due to phenological differences between varieties on a given date. These were: 3rd leaves unfolded (14), inflorescences clearly visible (53), inflorescences swelling and flowers closely pressed together (55), inflorescences fully developed and flowers separating (57), beginning of flowering: 10% of flowerhoods fallen (61), flowering (70), berries pea-sized and bunches hang (75), berry development (76), berries beginning to touch (77) and beginning of ripening (81). Full details of varieties, dates of measurements and growth stages are given in Table 1.

Table 1. Plot characteristics and phenological stages (BBCH scale) for each measurement dates 2016 and 2017 trials.

Block ID	Variety	Dates – 2016			
		T1: 03/05/2016	T2: 25/05/2016	T3: 23/06/2016	T4: 18/07/2016
Collection	*Marselan*	55	57	75	77
Faysse	*Chardonnay*	53	57	77	77
Franquet	*Cabernet Sauvignon*	14	55	75	77
Verdot	*Petit Verdot*	53	57	75	77
		Dates – 2017			
		T1: 28/04/2017	T2: 22/05/2017	T3: 14/06/2017	T4: 31/07/2017
Aranel	*Aranel*	57	62	75	81
Marselan	*Marselan*	57	61	75	81
Caladoc	*Caladoc*	57	61	75	81
PetitVerdot	*Petit Verdot*	57	62	75	77
Syrah	*Syrah*	57	61	75	85

2.2. Sprayer characteristics

An air-assisted side-by-side sprayer (Precijet, Tecnoma ®, Epernay, France) with nozzles set on vertical booms in front of each side of the canopy was used for all trials. Each boom was fitted with four hollow cone nozzles (TXA800067VK, Teejet, Wheaton, USA) aligned in a vertical plane to spray

6

157 the entire canopy. The Precijet is a more efficient sprayer than the pneumatic arch-type sprayers more

158 commonly used in the vineyards of southern France. For each spraying date and each block, sprayer

159 settings (number and direction of nozzles) were adapted according to the canopy size following good

160 agricultural practices and were not altered from one sampling site to another during block spraying. At

161 all dates and blocks, the working pressure was 0.5 MPa and the total flow rate was 5.5 L min^{-1}. At a

162 forward speed of 5 km h^{-1} the spray volume was 150 L ha^{-1}.

163

164 ***2.3. Data collection***

165

166 *2.3.1. Measurements of spray deposition*

167

168 For each date and each block, a 15 m section of a vineyard row was chosen under two constraints; i)

169 that it represented typical growth for the phenological stage and ii) that it was as homogeneous as

170 possible, i.e. sections with missing, over vigorous or under vigorous vines were avoided. Spray

171 deposition for each application was determined by including a chemical tracer in the spray application

172 and embedding part of the 15m section with artificial collectors. Different 15 m long sections were

173 chosen from one date to another to ensure that measurements were not affected by previous survey

174 activities.

175

176 The deposition sampling scheme differed slightly for the two years. In 2016, four consecutive vines

177 segments were sampled within each 15 m section. On each vine segment, 0.004 m² polyvinyl chloride

178 (PVC) collectors were positioned on the leaves inside the canopy in several planes according to a

179 profile perpendicular to the row according to a cell grid 0.2 m high and 0.1 m wide. In 2017, two

180 three-vine segments (that were termed a "trio") were sampled within each 15 m section. Within each

181 trio, a regular grid of the 0.004 m² PVC collectors was established in several planes; however, at a

182 lower density with a spacing of 0.4 m vertically and 0.1 m horizontally. Each trio in 2017 and each

183 four-vine section in 2016 will be called hereafter a "sampling unit". Details of the number of collectors

184 analysed for each sampling unit at each sampling date are given in Table 2.

7

185

Table 2. Number of collectors sampled (with spray deposits) in 2016 and 2017 for each sampling unit selected within the 15 m long plots. In 2016 there was one 4-vine section per 15 m and in 2017 there were two 3-vine sections sampled per 15 m of vine row.

Block ID	Sampling unit ID	Dates - 2016			
		T1: 03/05/2016	T2: 25/05/2016	T3: 23/06/2016	T4: 18/07/2016
Collection	A	28	95	109	117
Faysse	B	30	61	65	101
Franquet	C	30	52	95	121
Verdot	D	30	62	120	101
		Dates - 2017			
		T1: 28/04/2017	T2: 22/05/2017	T3: 14/06/2017	T4: 31/07/2017
Aranel	A1	34	37	71	66
	A2	29	51	69	72
Marselan	B1	24	46	68	66
	B2	27	50	66	67
Caladoc	C1	32	47	67	69
	C2	28	48	65	59
PetitVerdot	D1	22	38	48	47
	D2	22	36	53	47
Syrah	E1	21	NA[†]	67	67
	E2	25	NA[†]	64	69

186 [†] No deposition data on the Syrah block on 22/05/2017 following a problem of accessibility to the
187 block due to phytosanitary treatments.

188
189 A quantitative assessment of the spray distribution in the canopy was made by measuring the

190 deposition of a colorimetric tracer, Tartrazine E-102 (Sigma, St. Louis, MO, USA) on the PVC

191 collectors (Codis et al., 2018). For each spray campaign, the sprayer was filled halfway with distilled

192 water and the necessary amount of Tartrazine was added to achieve a target concentration of 10 g. L^{-1}.

193 This solution was then sprayed, reproducing normal spraying procedures. After the tracer had

194 completely dried, all PVC collectors were retrieved and placed in individual bags. In the laboratory,

195 each individual PVC collector was rinsed in a known volume of distilled water to recover the

196 Tartrazine and the concentration was measured with a spectrophotometer at 427 nm (Uviline 9100,

197 resolution: 0.001, accuracy ± 0.003, Secomam, Champigny sur Marne, France). Deposition was

198 normalised according to the collector surface and to the Tartrazine dose rate ha^{-1}. Spray deposits were

8

199 expressed in nanograms per square decimetric of leaves for 1 g sprayed ha^{-1} (ng dm^2 per 1g ha^{-1})

200 (Codis et al., 2018).

201 It should be noted that many physical effects influence deposition values, including variation in the

202 spray trajectory angle, anisotropic leaf area distribution, streamlining of leaves in the air flow and

203 small-scale aerodynamics of spray droplets (Walklate et al., 2011). These effects are either considered

204 constant or impractical to measure. The sampling design, based on a regular 2D grid across the canopy

205 row along a minimum length of 3 m of vine row, was designed to minimise any of these potential

206 effects.

207

208 Artificial collectors are often used as replacements for natural foliage in research studies as the

209 recovery of sprayed tracer retained on natural plant surfaces is more difficult and more expensive than

210 from artificial targets. Furthermore, research using natural targets is always limited by the size and

211 spatial heterogeneity of the sample, and these parameters play an important role in the unbiased

212 estimation of deposition in vegetation (Forster et al., 2014). PVC collectors have been demonstrated to

213 have a good recovery rate and are efficient in recovering the spray deposits (Garcerá et al., 2012).

214 From the results presented in the literature, this study used the hypothesis that the distribution of

215 deposits intercepted on PVC collectors is near to the distribution actually observed on vine leaves.

216

217 Historically, deposits onto vine leaves or PVC collectors (Codis et al., 2018), have been aggregated to

218 give a mean deposition per sampling unit, without taking into account the variability or spatial

219 distribution of deposition rates within the sampling unit. However, in order to ensure optimal crop

220 protection, it is assumed here that the attribute space can be characterised more precisely by a

221 statistical distribution rather than a mean. Using the statistical distribution, rather than a mean of

222 deposition, makes it possible to account for the variability of locally intercepted deposits and to avoid

223 PPP under-dosing, regardless of the area in the canopy where this under-dosing may occur.

224

225 As the intent here is to examine if and how spray deposition varies within the canopy, the distribution

226 of deposits across all vineyards for each individual survey (date) were aggregated and described using

9

227   deciles. It is worth noting that although the PVC collectors were located in a regular 2D grid across the

228   canopy, their physical location has not been explicitly used in the modelling. The crop management

229   hypothesis is that if the attribute space can be modelled more accurately with a statistical distribution

230   rather than a mean, then management can be altered to avoid under-dosing, regardless of where it

231   occurs in the canopy.

232

233   *2.3.2. 2D LiDAR information of canopy structure*

234

235   A Sick LMS100 (SICK AG, Düsseldorf, Germany) 2D LiDAR sensor was used in the study. The

236   LMS100 is a fully-automatic divergent laser scanner based on time-of-flight (TOF) measurement with

237   a typical error of ± 30mm, a selectable angular resolution ($\Delta\theta$) set to 0.5° and a range of 270°. With

238   these settings, there were 541 distances recorded for one complete laser rotation, which is hereafter

239   referred to as a "scan", and scans were obtained at 50 Hz. The LMS100 and data logging system were

240   mounted on a purposely-built stainless-steel mast fixed behind the tractor operating the sprayer,

241   according to a previously described procedure (Cheraiet et al., 2020). The LMS100 sensor height

242   ranged from 1.0 – 1.4m above ground level and was adjusted up during the season to account for

243   increasing canopy height. The tractor was driven along the vineyard rows at a constant forward travel

244   speed of 5 km h^{-1}, with a typical error of ± 0.21 km h^{-1} (IFV, internal report, October, 2018).

245

246   This sensing system was coupled to a Real Time Kinematic (RTK) GNSS receiver (Teria GSM

247   correction, Vitry-sur-Seine, France) to identify the start and end point of the sampling units. Once the

248   starting point was set, scans were aggregated using a fixed forward distance based on the constant

249   tractor speed to generate a 3D point cloud reconstruction of the vine environment. The sprayer

250   replicated commercial operations, i.e. the tractor only traversed every second row so that the canopy

251   was only scanned from one side. This differs to most previous research activities with LiDAR sensors,

252   but was deliberately done to approximate commercial conditions. Full details of the system set-up are

253   given in Cheraiet et al. (2020).

254

255   *2.3.2.1. Derivation of primary canopy attributes*

256

257   The determination of primary canopy dimensions (height and width) from the filtered LiDAR data was

258   performed using the LiDAR bayesian point cloud classification algorithm (BPCC) (Cheraiet et al.,

259   2020). This is achieved by (a) a 1D cluster analysis of the LiDAR point clouds to identify different

260   components of the vine and trellis system (trunk, vegetation zone, trellis wire), followed by a Bayesian

261   classification, and (b) an estimation of canopy height and width using an adjustable statistical

262   threshold to improve canopy dimension estimates as the canopy develops. For canopy width, the

263   method derives a half-vine width, as only one side of the canopy is scanned, and assumes symmetry to

264   derive the full vine canopy width. Full details of the BPCC method are in Cheraiet et al. (2020).

265

266   Several indicators for vegetation density based on 2D LiDAR acquisition have previously been

267   proposed but have drawbacks for use in predicting deposition distributions in the canopy. The density

268   metric proposed by Llorens et al. (2011b) exhibits a strong collinearity with vegetation height and is

269   discrete in nature (5 classes), making it less suitable for modelling. The tree area index (TAI) proposed

270   by Walklate et al. (2002) has been shown to be sensitive to the length of the vine row section scanned

271   and is only recommended for > 1 m row sections (Arnó et al., 2013). This limits its usefulness for

272   multi-scale dose modulation methods, especially if real-time and high resolution dose modulation are

273   to be considered. Therefore, an adapted estimation of canopy density using LiDAR data, called the

274   intercepted beam rate (IBR), is proposed here. The IBR is similar to the metric of Llorens et al.

275   (2011b) except that it is restricted to interceptions in the canopy zone defined by the BPCC algorithm.

276   It is expressed as a continuous value, not a class, generating more degrees of freedom to characterise

277   heterogeneity in the canopy density. The IBR (%) is defined as (Eq. 3):

278

279     $$IBR = \frac{NBI}{NBE} * 100$$ Eq. 3

280   Where: NBI is the number of beams intercepted between angles that define the range of the canopy

281   zone height along a trellis and NBE is the total number of beams emitted over the same angular range.

282   The mean IBR was calculated for each sampling unit.

283

284   *2.3.2.2. Integrated indicator: Leaf Wall Area*

285

286   The LWA is the area of leaf based on the assumption that the canopy sides are completely flat, and

287   hence, form a "wall". The LWA has been chosen at the European Union level as the new metric to

288   support dose expression in 3D cropping systems when performing efficacy trials during registration

289   processes (EPPO, 2016). The LWA is expressed in square metres per hectare (m² ha^{-1}) and defined as

290   (Eq. 4):

291

292     $$LWA = \frac{2 \times VH \times 10,000}{RS}$$ Eq. 4

293   Where: VH is canopy height (m); 10,000 is the ground area (m²) and RS is the row spacing (m).

294

295   The LWA is derived from canopy height and row spacing only, with the later usually a constant in

296   vineyards. Therefore, while LWA is considered an integrative metric, it is directly correlated to

297   canopy height. Canopy width and density information is not included.

298

299   **2.4. Modelling**

300

301   Previous approaches to modelling intercepted spray deposits within a crop canopy have used power

302   (Bastianelli et al., 2017) or logarithmic (Siegfried et al., 2007) laws to model mean depositions. As the

303   intent here is model deposition distribution, not mean deposition, log-lin regression models were used

304   to improve model behaviour and fitting at the upper and lower limits of the distribution.

305

306   The data acquired on the 2017 and 2016 plots were used as calibration and validation sets respectively.

307   The 2017 data was used for calibration as it had a higher number of PVC collectors per sampling unit

308   (Table 2) and the 2017 survey encompassed a longer phenological period (Table 2). The calibration

309   data were used to develop both univariate and multivariate regression models for predicting foliar

310   deposits distributions, while the validation data were used to evaluate the performance of the

311   developed models.

312

313   Univariate empirical models for the prediction of foliar deposit distributions were derived using the

314   integrative indicator (LWA) as the sole predictor. This formed a "standard" model based on the

315   current European standard. For each decile of the deposition distribution, a log-lin regression model

316   was used (Eq. 5).

317

318
$$y_{i,j} = U_j e^{-(\eta_j * LWA_i)} + e_{i,j}, \ \ y_{i,j} > 0 \tag{Eq. 5}$$

319   Where: $y_{i,j}$ represents the value of the jth decile of spray deposit in the ith vine trio with $\forall i \in [1, 40]$

320   and $\forall j \in [1,9]$, e_i are random variables, it is assumed that e_i are independent and $\varepsilon_i \sim N(0, \sigma^2)$, LWA_i

321   is the leaf wall area for the sample site in the ith sampling unit, U_j and η_j are real unknown parameters

322   that will have to be estimated, where U_j is the intercept and η_j is the slope of the model equation for

323   the prediction of jth decile.

324

325   Multivariate models for prediction of decile deposition as a linear combination of primary canopy

326   attributes (VH, VW and IBR) were similarly constructed using the same log-lin model form (Eq. 6).

327

328
$$y_{i,j} = M_j e^{-(\alpha_j * VH_i + \beta_j * VW_i + \gamma_j * IBR_i)} + e_{i,j}, \ \ y_{i,j} > 0 \tag{Eq. 6}$$

329   Where: $y_{i,j}$ represents the value of the jth decile of spray deposit present in the ith vine trio with $\forall i \in$

330    $[1, 40]$ and $\forall j \in [1,9]$, e_i are random variables, it is assumed that e_i are independent and

331    $\varepsilon_i \sim N(0, \sigma^2)$, VH_i is the mean value of vegetation height measured at the ith vine trio, VW_i is the mean

332   value of vegetation width measured at the ith vine trio, IBR_i is the mean value of intercepted beam rate

13

333   measured at the ith vine trio, M_j, α_j, β_j and γ_j are real unknown parameters to be estimated, where M_j

334   is the intercept and $\alpha_j, \beta_j, \gamma_j$ are the slopes corresponding respectively to VH, VW and IBR in the

335   model equation for the prediction of jth decile.

336

337   A stepwise forward approach was used to identify the most parsimonious prediction model (uni-, bi-

338   or tri-variate) as well as the statistical weight of each predictor in the models. Models for each

339   deposition decile were ranked using the corrected Akaike's Information Criterion (AICc) as the

340   number of data were limited (≤ 40 data points) (Hurvich and Tsai, 2001).

341

342   Multicollinearity among the explanatory variables was tested using the variance inflation factor (VIF)

343   (Akinwande et al., 2015) (Eq. 7): The VIF was calculated for each multivariate model used to predict a

344   decile deposition and VIF > 5 set as a threshold to indicate relatively high levels of multicollinearity in

345   the models.

346

347
$$VIF = \frac{1}{1-R^2} \qquad \text{Eq. 7}$$

348   Where: R^2 is the coefficient of determination of the prediction model.

349

350   ***2.5. Model Evaluation***

351

352   The coefficient of determination (R²) and the normalised root mean square error (nRMSE) were used

353   to evaluate the fit of the calibration models (2017 data). The nRMSE was used to facilitate comparison

354   between models of all the deposition deciles and is defined as a percentage (Eq. 8):

355

356
$$nRMSE_j = \frac{\sqrt{\sum_{i=1}^{N} \frac{(\hat{y}_{i,j} - y_{i,j})}{N}}}{\bar{y}_{i,j}} * 100 \qquad \text{Eq. 8}$$

357   Where: $\hat{y}_{i,j}$ are estimated values for the jth decile, $y_{i,j}$ are observed values for the jth decile and $\bar{y}_{i,j}$ are

358   the mean of observed values for the jth decile, and N is the number of observations.

359

360   The performance of the univariate and multivariate decile models, when applied to the validation data,

361   was assessed by analysing the observed vs. predicted values by the (i) R² of a 1:1 linear regression fit,

362   (ii) model bias (%) and, (iii) normalised root mean square error of prediction (nRMSEp) (normalised

363   by the mean of the predicted decile deposit values). Again the nRMSEp is defined as a percentage (Eq.

364   9):

365

366    $$nRMSEp_j = \frac{\sqrt{\sum_{i=1}^{N} \frac{(Y_{i,j} - y_{i,j})}{N}}}{Y_{i,j}} * 100$$ Eq. 9

367   Where: $Y_{i,j}$ are predicted values for the jth decile, $y_{i,j}$ are observed values for the jth decile and $\bar{y}_{i,j}$ are

368   the mean of predicted values for the jth decile, and N is the number of observations.

369

370   All analyses were performed using the open source statistical R Software® (Version 1.2.5001) (R

371   Development Core Team, 2020). Respectively, for the AIC, nRMSE and VIF calculations, the stats4

372   (version 3.6.2), Metrics (version 0.1.4), car (version 3.0.10) packages were used.

373

374   **3.   Results and discussions**

375

376   *3.1. Data description*

377

378   *3.1.1. Description of the deposition data*

379

380   The deposition distributions exhibited a positive skewness, associated with very high deposition rates

381   on the external canopy PVC collectors. The 10th decile skewed the distribution and was characterised

382   by oversaturation relative to the target dose. It is commonly accepted by growers and experts that the

383   external canopy layers that face the sprayer will exhibit this phenomenon to achieve adequate

384   deposition in the internal layers. As oversaturation is assumed to ensure protection, the 10th decile was

385   excluded from subsequent analyses and only the first nine deciles were used for modelling.

386

15

387   The empirical density curve of the depositions recorded by the PVC collectors positioned within the

388   vine trios in 2017 showed a clear trend towards a decrease in mean deposition associated with

389   increasing vine growth over time that is being sprayed with a constant quantity of tracer (Fig. 1). The

390   deposition distributions followed a Poisson-type form and the shape of the distribution changes over

391   time, with the mean and the variance decreasing as the season progresses. The median foliar

392   deposition ranged from 500 ng dm² per 1g ha^{-1} in T1 to 195 ng dm² per 1g ha^{-1} in T4.

393

394   Figure 1 near here

395

396   The Poisson distributions indicated that a unique and central statistic (mean or median) of the deposit

397   was insufficient to describe the data, even if completed by a quantification of variance. This highlights

398   the problem of modelling deposition using the mean and supports the use of the decile by decile

399   analysis in order to take into account the statistical dispersion of deposition values.

400

401   Deposition rates also varied between varieties at a given date, with inter-block variability being

402   greatest early in the season (at T1, 38%) and lowest at the latest observation (T4, 11%) (data not

403   shown). This can be explained by differences in the timing of bud-burst and shoot development

404   between the grape varieties early in the season (Table 1). Even at full canopy development (T3-T4),

405   some differences in shoot length, leaf size and shape and vine morphology between varieties still

406   existed, despite the common trellising systems between vineyards.

407

408   *3.1.2. LiDAR-derived canopy data*

409

410   Summary plots of the primary canopy attributes (VH, VW and IBR) derived from the LiDAR sensor

411   survey in the 2017 survey blocks, at a resolution scale of 3 m (same as vine trio scale used for

412   sampling deposits) are shown in Figure 2.

413

414   Figure 2 near here

415

416   Table 3. Summary of canopy height (VH) and width (VW) and density (IBR) data obtained at the four

417   LiDAR acquisition dates in 2017.

	T1	T2	T3	T4
Vegetative parameters	Mean			
VH (m)	0.65	0.99	1.24	1.19
VW (m)	0.38	0.59	0.83	0.81
IBR (%)	28.2	45.3	59.1	72.4
	CV (%)			
VH	13.1	14.5	16.2	17.1
VW	10.2	16.6	11.5	5.3
IBR	9.4	12.7	12.3	19.6

418

419   Vegetation height and width (Figs. 2a-b) increased almost linearly from bud break (T1) to green pea

420   stage (T3), which is approximately the date of the first canopy trimming operation. Trimming,

421   combined with increasing water stress over summer, tends to stagnate any further growth. This is

422   reflected in a plateauing of VH and VW between T3 and T4 (Table 3), which indicated that these

423   parameters were likely to be less informative about changes in canopy conditions towards the end of

424   the season. Overall, the earlier varieties (Aranel, Marselan and Caladoc) had larger dimensions than

425   the later developing variety (Petit Verdot) that never caught up in size to the other varieties (Figs. 2a-

426   b). On average, over the survey period (T1-T4), the inter-block variability was 15.2% and 11% for VH

427   and VW respectively. This showed that there were real differences between blocks during the growing

428   season (Table 3).

429

430   In contrast to VH and VW, the IBR canopy density metric (IBR) did not plateau in any block between

431   T3 and T4, despite the in-season canopy trimming operations (Fig. 2c). This indicated that IBR could

432   provide relevant information to characterise the canopy later in the season. The variability of the IBR

433   metric also increased as the season progressed, with the IBR parameter having a CV of 9.4% in T1,

434   12.7% in T2, 12.3% in T3 and 19.6% in T4 (Table 3). This higher variability of the mid- to late-season

435   IBR corresponds to the period when mean deposits were lowest (Fig. 1).

436

3.2. Modelling

3.2.1. Univariate models

The results of the univariate model construction for deciles 1-9 (D1-D9) with the calibration data set

showed a relatively stable relationship ($0.69 < R^2 < 0.82$) for the prediction of foliar deposition using

the LiDAR-derived LWA indicator (Table 4). The first two deciles (D1-D2) had the lowest prediction

quality (R^2) and the greatest error of the prediction models (nRMSE) (Table 4). The mean deposition

was also modelled, which is the current recommended approach, and explained 80% of the variance in

the mean deposition in the canopy.

Table 4. Parameters and quality indicators of univariate models for prediction of decile deposition over the entire growing season: indicating model coefficients (U and λ) and quality indicators for each decile model for both the calibration (R^2 and nRMSE) and validation (R^2 of 1:1, nRMSE and bias) stages. The equivalent mean model (current standard reference) parameters and quality indicators are also shown.

Deciles distribution deposit	Model equation		Calibration (2017) (n=40)		Validation (2016) (n=16)		
	U	λ	R^2	nRMSE (%)	R^2 of 1:1 line	nRMSEp (%)	Bias (%)
D_1	740.6	2.35E-04	0.69	46	0.66	45	-5.8
D_2	935.39	2.54E-04	0.75	36	0.77	41	-4.8
D_3	1282.13	2.61E-04	0.79	28	0.80	37	-3.9
D_4	1524.34	2.58E-04	0.81	25	0.75	34	-2.3
D_5	1702.88	2.47E-04	0.81	19	0.80	30	2
D_6	1820.63	2.35E-04	0.78	17	0.82	27	2.9
D_7	2100.3	2.30E-04	0.80	18	0.83	25	2.1
D_8	2474.84	2.25E-04	0.79	20	0.85	29	7.6
D_9	3045.88	2.19E-04	0.82	21	0.81	34	8.4
mean	1789.88	2.40E-04	0.80	18	0.79	26	2.2

Applying the calibrated model to the independent validation data (2016) generated prediction

accuracies for the univariate decile models that were similar to and followed the same trend as the

calibration models ($0.66 < R^2 < 0.85$), with lower deciles being associated with lower prediction

452   quality (Table 4). The bias values were negative for the validation models predicting deciles D1 to D4

453   and positive for deciles D5 to D9 (Table 4). The lower deciles represent areas of the canopy where a

454   below mean level of deposition was achieved, which may be insufficient for effective crop protection.

455   In these deciles, the univariate model underestimated (negative bias) depositions in the already poorly

456   covered (low deposition) areas.

457

458

459   Figure 3 near here

460

461   The model fit for the median deposition (D5) is shown as an example (Fig. 3). The overestimation at

462   higher deposition rates, associated with T1 (red squares; early season), is evident. Correct application

463   of early season PPPs is important for prophylactic protection of the plant and a systematic

464   overestimation of deposition is undesirable. However, when the canopy is small (early season), the

465   median depositions were very high (Fig. 1), so with a fixed dosage per hectare there is little risk of

466   under-application. This may change if dose expression regulations are altered in the future to minimise

467   the risk of early season over-applications and to improve the use-efficiency of PPPs. For T2, T3 and

468   T4, the median deposition from the model underestimated real conditions, i.e. it was likely that there

469   was more being applied than was being modelled. However, under the fixed dose expression

470   regulations, the amount of deposition per canopy surface area was dropping as the canopy increased,

471   so under-applications are more likely. Underestimation is preferable to overestimation under these

472   conditions, although correct estimation is preferred. The ability of the univariate model to robustly

473   predict median foliar deposition throughout the growing season was not assured. This can be

474   explained by the fact that the univariate approach only accounted for VH in the LWA, but not VW or

475   canopy density.

476

477   *3.2.2. Multivariate models*

478

479 The VIF analysis indicated that there was no multicollinearity (VIF < 5) between the primary canopy

480 attributes (VH, VW and IBR) in the multivariate decile deposition models. The stepwise parameter

481 selection showed that the IBR metric had the strongest contribution to the D1-D3 models, followed by

482 VW and then VH. Thus for low deposition values, which are more common at the end of the growing

483 season (T3 and T4), the IBR was dominant for predicting deposition (Table 5). For the D7-D8

484 prediction models, which corresponded to high deposition values, VH and VW were the strongest

485 predictors, followed by IBR (Table 5). Therefore, when the canopy was developing (T1 and T2)

486 information on VH and VW was important for modelling deposition. Once the canopy had reached

487 full size (T3 and T4) and VH and VW had stabilised, the importance of VH and VW diminished.

488

Table 5. Multivariate models for predicting of decile deposition: comparison of the relative weight
(order of occurrence in the model (1, 2 or 3)) of the primary canopy attributes (VH, VW and IBR)
according to the conditional Akaike information criterion and study of the multi-collinearity between
the primary canopy attributes by variance inflation factor (VIF).

Deciles model	Primary canopy attributes					
	vegetation height (VH)		vegetation width (VW)		Intercepted beam ratio (IBR)	
	order of occurrence in the model	VIF	order of occurrence in the model	VIF	order of occurrence in the model	VIF
1	3	1.63	2	1.59	1	2.09
2	3	2.13	2	2.34	1	2.02
3	3	1.81	2	2.98	1	2.67
4	2	3.22	1	3.74	3	3.06
5	2	3.32	1	3.45	3	2.06
6	2	3.35	1	3.75	3	1.61
7	1	2.78	2	2.1	3	1.94
8	1	2.37	2	3.36	3	1.62
9	1	3.53	2	3.74	3	2.53

489

490 The parameters for the fitted multivariate calibration models and model statistics for both the

491 calibration and validation models are shown in Table 6. Prediction quality was very good for both the

492 calibration ($0.81 < R^2 > 0.93$) and validation ($0.79 < R^2 > 0.94$) data sets and these followed the same

493 trend as the univariate approach, with lower fits at lower deciles. The nRMSE ranged from 22% to 7%

for calibration and 24% to 10% for validation (Table 6). The validation bias was negative for all nine

prediction models (Table 6), indicating that the multivariate deposition decile models underestimated

deposition for all deciles in the distribution. While underestimation was not desirable, a "worst-case"

risk management modelling approach should encourage underestimation rather than overestimation of

deposition, in order to ensure that PPPs are applied in sufficient quantity. Figure 4a shows the

relationship between the observed and predicted median (D5) deposition for the multivariate case

(comparable to the univariate case in Fig. 3). The data plots close to the 1:1 line, over the entire period

of the study (T1 – T4), but consistently slightly underestimates depositions (Fig. 4a). The ability of the

multivariate model to reliably predict median foliar deposition throughout the growing season was

explained by its ability to account for the differential contribution of VH, VW and IBR to deposition

as the canopy develops. The actual log-lin regression for the median deposition prediction model (D5),

using the model parameters in Table 6, is shown in Figure 4b as an example.

Table 6. Parameters and quality indicators of multivariate models for prediction of decile deposition over the entire growing season: including model coefficients (M and α, β, γ) and quality indicators for each decile model for both the calibration (R^2 and nRMSE) and validation (R^2 1:1, nRMSE and bias) stages (same as Table 4). Decile 10 is not shown.

Deciles distribution deposit	Model equation				Calibration (2017) (n=40)		Validation (2016) (n=16)		
	M	α	β	γ	R^2	nRMSE (%)	R^2 of 1:1 line	nRMSEp (%)	Bias (%)
D_1	847.32	1.06	0.3	1.28	0.81	22	0.79	24	-1.5
D_2	1057.31	0.97	0.48	1.13	0.83	20	0.81	21	-2.1
D_3	1506.97	0.82	0.37	1.54	0.88	10	0.83	15	-2.2
D_4	1819.9	0.7	0.36	1.69	0.92	9	0.87	12	-2.5
D_5	2055.62	0.55	0.34	1.81	0.93	9	0.94	13	-2.1
D_6	2154.46	0.52	0.47	1.59	0.88	7	0.91	10	-2.6
D_7	2530.31	0.38	0.43	1.77	0.91	8	0.9	12	-3.1
D_8	2976.56	0.34	0.46	1.75	0.9	10	0.9	13	-2.8
D_9	3578.82	0.39	0.55	1.5	0.91	11	0.89	14	-3.2

Figure 4 near here

3.3. Assessment of the performance of multivariate models compared to univariate models

For all decile levels, the multivariate model outperformed the univariate model (higher R^2, lower nRMSE) (Tables 4 and 6). The improved performance of the multivariate models was attributed to the additional information on canopy width and density available to the model, both of which influence deposition. The bias of the multivariate models was always negative (Table 6), unlike the univariate prediction models of deciles D5 to D9 that had a positive bias (Table 4). The overestimation of deposition at the early stages of the growing season, when the risk of pathogen occurrence and development is highest, is not problematic under current fixed dose regulations, as the real deposition rates are very high (Fig. 1). For systems where the dose expression is adjusted to expected canopy size, overestimation may be an issue and the use of the LWA to determine the dose to be applied presents a potential risk of underdosing (Rüegg et al., 2001). This would have potential consequences on the efficacy of PPP. These models need to be tested under these conditions, but the results here indicated that the multivariate model provided a more risk-adverse model for managing plant protection risk throughout all stages of the growing season. Thus, multivariate statistical models offer the possibility to react to the evolution and variability of vegetation during the season, so that it is possible to consider reducing the use of PPPs while providing a margin of safety to growers in terms of crop protection.

The low deposition values that constituted (D1-D4) were found at all four dates (T1 to T4) (Fig. 1). Therefore, the prediction models for D1-D4 take into account deposition data from all dates (T1 to T4), which may lead to these prediction models having poorer quality with regards to accuracy and uncertainty. In contrast, higher deposition values (greater than 500 ng dm² per 1g ha^{-1}) were only found at T1 and T2.

3.4. Potential uses of multivariate deposit prediction models

537   The current use of a fixed dose expression under European guidelines, which is independent of canopy

538   size, is problematic. Guidelines are evolving and a first step toward this was the introduction of the

539   LWA metric into calculations of dose expression in all situations (EPPO, 2016). However, this new

540   LWA-based dose expression is based on the unproven hypotheses that (i) dose requirements are a

541   function of a single integrative indicator and (ii) there is a strictly linear relationship between

542   intercepted deposits and the quantity of vegetation canopy to be protected. The results from this study

543   indicated that this relationship was not necessarily linear and that using individual canopy attributes in

544   a multivariate model, rather than an aggregated canopy metric, provided more flexibility in the

545   modelling process. As vine canopies evolve, the relative importance of different canopy dimensions

546   for modelling depositions also changed. This flexibility and improve modelling will become more

547   important if dose expression shifts from an analysis of mean deposition rates to an analysis of the

548   expected distribution of deposition rates within a canopy. From the perspective of commercial

549   applications, this is unlikely to become the norm in the near future; however, from a regulatory

550   perspective and for testing and grading the performance of new commercial sprayers, the ability to

551   better model the distribution of depositions will be very useful in promoting more effective and

552   efficient spray systems.

553

554   Ultimately the ability of these, or similar, multivariate models will make it possible to consider a step

555   change in the spray management paradigm from managing a mean deposition (Walklate et al., 2011)

556   to managing the deposition distribution at any given time over the season. This will allow deposition

557   in areas of the canopy that are least well treated (D1-D2) during a spray operation to be taken into

558   account. The decomposition of the overall deposition into a distribution will be critical to a better

559   epidemiological understanding of resistance and pathogen pressure after phytosanitary treatments have

560   been carried out. In this study, the distribution has only been described in the attribute space, and not

561   in the geographical (canopy) space. It is expected that the areas of lower deposition will be located in

562   denser areas of the canopy with greater numbers of leaf layers between the target point and the

563   sprayer; however, more research is certainly needed to develop approaches to spatialise the

564   distribution of deposits within the canopy.

565

566   Furthermore, in view of the quality of the prediction models developed in this study at a trio scale (3m

567   of trellised vineyard row), the application of these multivariate prediction models at such a small

568   spatial scale offers interesting possibilities for the optimization of spraying in viticulture. If high-

569   resolution spatial canopy dimensions, including density, are generated, then differential or variable-

570   rate spraying could be performed in real-time. This can be achieved by sensing pre-spraying to

571   develop prescription spray maps, or by sensing directly in front of a sprayer to perform real-time dose

572   modulation (Llorens et al., 2010). The proposed modelling approach here, when tuned to sprayer

573   characterisers, could be used to model and optimise deposition coverage whilst minimising the

574   quantity of PPP applied. This is a clear objective for the industry (EPPO, 2016) and is not just

575   dependent on good sensing and variable-rate technology but also on good decision support systems

576   that require accurate predictive modelling capabilities. In addition to supporting differential spraying,

577   improved deposition models could be applied site-specifically post-application to identify areas where

578   the PPP application may have been sub-optimal i.e. where there is a disagreement between the amount

579   applied and the amount modelled.

580

581   **4. Conclusions**

582

583   Optimization of the use of crop protection inputs in viticulture should take into account the structural

584   characteristics of the vegetation. In this study, a multivariate statistical modelling approach was

585   proposed to predict the mean and distribution of spray depositions as a function of primary vine

586   canopy attributes (height, width and density) that were derived from a LiDAR sensor system. Results

587   obtained from data collected over two years, on seven grape varieties and on two trellising systems,

588   showed that the proposed multivariate statistical models can predict the distribution of depositions of a

589   typical face-to-face sprayer more accurately and robustly than univariate prediction models based on a

590   calculation of leaf wall area, the current industry standard. This ability to predict deposition

591   distributions will allow areas of the vine canopy that are poorly treated (unprotected) after spraying to

592   be taken into account and will provide a better understanding, from an epidemiological point of view,

593 of resistance and pathogen pressures in vineyards. In addition, the results provided clear indications of

594 the ability of multivariate statistical models to react to changing canopy attributes over the season and

595 spatially in the vineyard, such that it is possible to envisage using these models for a site-specific

596 reduction in the PPP expected by the wine industry while guaranteeing a safety margin for growers

597 when spraying.

598
599 **Acknowledgments**

600

609

610 **References**

611

612 Akinwande, M. O., Dikko, H. G., Samson, A. (2015). Variance inflation factor: as a condition for the

613   inclusion of suppressor variable (s) in regression analysis. Open Journal of Statistics, 5(07), 754.

614   https://doi.org/10.4236/ojs.2015.57075

615 Arnó, J., Escolà, A., Vallès, J. M., Llorens, J., Sanz, R., Masip, J., Palacín, J., Rosell-Polo, J. R., 2013.

616   Leaf area index estimation in vineyards using a ground-based LiDAR scanner. Precision

617   Agriculture, 14(3), 290-306. https://doi.org/10.1007/s11119-012-9295-0

618 Bastianelli, M., Rudnicki, V. D., Codis, S., Ribeyrolles, X., Naud, O., 2017. Two vegetation indicators

619   from 2D ground Lidar scanner compared for predicting spraying deposits on grapevine.

620   Proceedings of the 2017 EFITA WCCA conference, Montpellier, France, 153-154.

621 Byers, R. E., Hickey, K. D., Hill, C. H., 1971. Base gallonage per acre. Virginia Fruit, 60(8), 19-23.

622 https://doi.org/10.1590/S0103-90162013000600003

623 Cheraiet, A., Carra, M., Lienard, A., Codis, S., Vergès, A., Delpuech, X., Naud, O., 2019.

624 Investigation on LiDAR-based indicators for predicting agrochemical deposition within a vine

625 field. In 12th European Conference on Precision Agriculture, Precision Agriculture '19 (July),

626 (Eds). J.V. Stafford, Wageningen Academic Publishers, 157-164. https://doi.org/10.3920/978-90-

627 8686-888-9_18

628 Cheraiet, A., Naud, O., Carra, M., Codis, S., Lebeau F., Taylor J. A., 2020. An algorithm to automate

629 the filtering and classifying of 2D LiDAR data for site-specific estimations of canopy height and

630 width in vineyards. Biosystems Engineering, 200, 450-465.

631 https://doi.org/10.1016/j.biosystemseng.2020.10.016

632 Codis, S., 2016. Stakes for a new model of dose expression in viticulture: advantages and points to be

633 taken into consideration. In Proceedings of the EPPO Workshop on harmonized dose expression

634 for the zonal evaluation of plant protection products in high growing crops, Austrian Agency for

635 Health and Food Safety Vienna,12-13.

636 Codis, S., Carra, M., Delpuech, X., Montegano, P., Nicot, H., Ruelle, B., Ribeyrolles, X., Savajols, B.,

637 Vergès, A., Naud, O., 2018. Dataset of spray deposit distribution in vine canopy for two contrasted

638 performance sprayers during a vegetative cycle associated with crop indicators (LWA and TRV).

639 Data Brief, 18, 415–421. https://doi.org/10.1016/j.dib.2018.02.012

640 Colaço, A.F., Molin, J.P., Rosell-Polo, J.R., Escolà, A., 2018. Application of light detection and

641 ranging and ultrasonic sensors to high-throughput phenotyping and precision horticulture: Current

642 status and challenges. Horticultural Research 5, 35. https://doi.org/10.1038/s41438-018-0043-0

643 Derksen, R. C., Zhu, H., Fox, R. D., Brazee, R. D., Krause, C. R., 2007. Coverage and drift produced

644 by air induction and conventional hydraulic nozzles used for orchard applications. Transactions of

645 the ASABE, 50(5), 1493-1501. https://doi.org/10.13031/2013.23941

646 EPPO (European Plant Protection Organization)., 2016. Conclusions and recommendations.

647 Workshop on harmonized dose expression for the zonal evaluation of plant protection products in

648 high growing crops. Vienne, 18–20 October 2016. Available online :

649   https://www.eppo.int/media/uploaded_images/MEETINGS/Conferences_2016/dose_expression/Co

650   nclusions_and recommendations.pdf (accessed on 11 November 2020).

651 Flint ML, van den Bosch R (1981) A history of pest control. In: Flint ML, van den Bosch R

652   (eds) Introduction to integrated pest management. Springer, Boston, 51–81. https://doi.

653   org/10.1007/978-1-4615-9212-9_4

654 Forster, W. A., Gaskin, R. E., Strand, T. M., Manktelow, D. W. L., Van Leeuwen, R. M. (2014).

655   Effect of target wettability on spray droplet adhesion, retention, spreading and coverage: artificial

656   collectors versus plant surfaces. NZ Plant Protection, 67, 284-291.

657 Garcerá, C., Moltó, E., Zarzo, M., Chueca, P. (2012). Modelling the spray deposition and efficacy of

658   two mineral oil-based products for the control of Aonidiella aurantii (Maskell). Crop Protection,

659   31(1), 78-84. https://doi.org/10.1016/j.cropro.2011.10.004

660 Gil, E., Campos, J., Ortega, P., Llop, J., Gras, A., Armengol, E., Salcedo, R., Gallart, M., 2019.

661   DOSAVIÑA: Tool to calculate the optimal volume rate and pesticide amount in vineyard spray

662   applications based on a modified leaf wall area method. Computers and Electronics in Agriculture,

663   160, 117-130. https://doi.org/10.1016/j.compag.2019.03.018

664 Hurvich, C. M., Tsai, C. L., 1993. A corrected Akaike information criterion for vector autoregressive

665   model selection. Journal of Time Series Analysis, 14(3), 271-279. https://doi.org/10.1111/j.1467-

666   9892.1993.tb00144.x

667 Koch, H., 1993. Application rate and spray deposit on targets in plants. In: ANPP/BCPC 2nd

668   International Symposium on Pesticides Applications, Strasbourg, France, 1, 175–182.

669 Llorens, J., Gil, E., Llop, J., Escolà, A., 2010. Variable rate dosing in precision viticulture: Use of

670   electronic devices to improve application efficiency. Crop Protection, 29(3), 239-248.

671   https://doi.org/10.1016/j.cropro.2009.12.022

672 Llorens, J., Gil, E., Llop, J., Escolà, A., 2011a. Ultrasonic and LiDAR Sensors for Electronic Canopy

673   Characterization in Vineyards: Advances to Improve Pesticide Application Methods. Sensors,

674   11(2), 2177-2194. https://doi.org/10.3390/s110202177

675 Llorens, J., Gil, E., Llop, J., Queraltó, M., 2011b. Georeferenced LiDAR 3D Vine Plantation Map

676   Generation. Sensors, 11(6), 6237-6256. https://doi.org/10.3390/s110606237

677   Lorenz, D. H., Eichorn, K. W., Bleiholder, H., Klose, U., Meier, U., Weber, E., 1994. Phänologische

678   Entwicklungsstadien der Weinrebe (Vitis vinifera L. spp. Vinifera). (Phenological stages of

679   grapevine (Vitis vinifera L. spp. Vinifera)). Viticultural and Enological Science 49, 66-70.

680   https://doi.org/10.1111/j.1755-0238.1995.tb00085.x

681   Moorthy, I., Miller, J. R., Berni, J. A. J., Zarco-Tejada, P., Hu, B., Chen, J., 2011. Field

682   characterization of olive (Olea europaea L.) tree crown architecture using terrestrial laser scanning

683   data. Agricultural and Forest Meteorology, 151(2), 204-214.

684   https://doi.org/10.1016/j.agrformet.2010.10.005

685   Palleja, T., Landers, A. J., 2015. Real time canopy density estimation using ultrasonic envelope signals

686   in the orchard and vineyard. Computers and Electronics in Agriculture, 115, 108-117.

687   http://dx.doi.org/10.1016/j.compag.2015.05.014

688   Pergher, G., Petris, R., 2008. Pesticide dose adjustment in vineyard spraying and potential for dose

689   reduction. Manuscript ALNARP 08 011. Agricultural Engineering International CIGR Journal, 10,

690   1-9.

691   R Core Team., 2020. R: A language and environment for statistical computing. R Foundation for

692   Statistical Computing, Vienna, Austria. URL http://www.R-project.org/

693   Rosell, J. R., Llorens, J., Sanz, R., Arnó, J., Ribes-Dasi, M., Masip, J., Escolà, A., Camp, F.,

694   Solanelles, F., Gràcia, F., Gil, E., Val, L., Planas, S., Palacín, J., 2009. Obtaining the three-

695   dimensional structure of tree orchards from remote 2D terrestrial LiDAR scanning. Agricultural

696   and Forest Meteorology, 149(9), 1505-1515. https://doi.org/10.1016/j.agrformet.2009.04.008

697   Rosell, J.R., Sanz, R., 2012. A review of methods and applications of the geometric characterization of

698   tree crops in agricultural activities. Computers and Electronics in Agriculture, 81, 124-141.

699   https://doi.org/10.1016/j.compag.2011.09.007

700   Rüegg, J., Siegfried, W., Raisigl, U., Viret, O., Steffek, R., Reisenzein, H., Persen, U., 2001.

701   Registration of plant protection products in EPPO countries: Current status and possible approaches

702   to harmonization. EPPO Bulletin, 31(2), 143-152. https://doi.org/10.1111/j.1365-

703   2338.2001.tb00983.x

704   Siegfried, W., Viret, O., Huber, B., Wohlhauser, R., 2007. Dosage of plant protection products

705   adapted to leaf area index in viticulture. Crop Protection, 26(2), 73-82.

706   https://doi.org/10.1016/j.cropro.2006.04.002

707   Solanelles, F., Escolà, A., Planas, S., Rosell, J. R., Camp, F., Gràcia, F., 2006. An Electronic Control

708   System for Pesticide Application Proportional to the Canopy Width of Tree Crops. Biosystems

709   Engineering, 95(4), 473-481. https://doi.org/10.1016/j.biosystemseng.2006.08.004

710   Vivier, M. A., Pretorius, I. S., 2002. Genetically tailored grapevines for the wine industry. Trends in

711   Biotechnology, 20(11), 472-478. https://doi.org/10.1016/S0167-7799(02)02058-9

712   Walklate, P. J., Cross, J. V., Richardson, G. M., Murray, R. A., Baker, D. E., 2002. Comparison of

713   different spray volume deposition models using LIDAR measurements of apple orchards.

714   Biosystems Engineering, 82 (3), 253–267. https://doi.org/10.1006/bioe.2002.0082

715   Walklate, P. J., Cross, J.V., Pergher, G., 2011. Support system for efficient dosage of orchard and

716   vineyard spraying products. Computers and Electronics in Agriculture 75, 355–362.

717   https://doi.org/10.1016/j.compag.2010.12.015

718   Walklate, P. J., Cross, J. V., 2012. An examination of Leaf-Wall-Area dose expression. Crop

719   Protection, 35, 132-134. https://doi.org/10.1016/j.cropro.2011.08.018
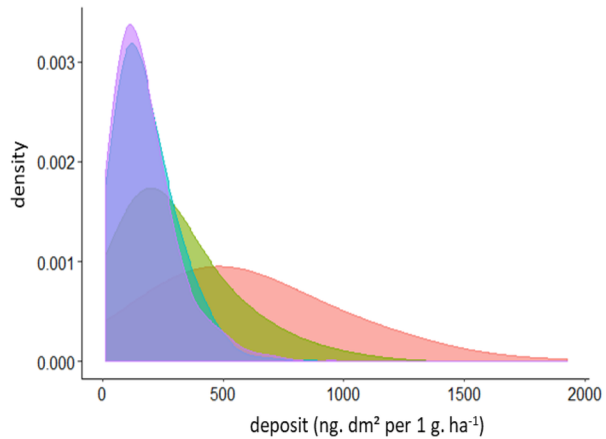
720

721   **Figures caption**

722

723   Figure 1. Empirical density curves of deposition values as a function of spray date (T1, T2, T3, T4)

724   obtained from 2017 calibration data.

725

726   Figure 2. Evolution of primary canopy attributes VH (A), VW (B) and IBR (C) at the vine trio scale

727   (shown as a dot on graphs) by blocks (Aranel (red), Caladoc (brown), Marselan (green), Petit verdot

728   (blue) and Syrah (purple)) over the entire growing season (T1 to T4) in 2017. At each date, a box plot

729   is presented in order to summarise the information obtained for the relevant primary canopy attribute.
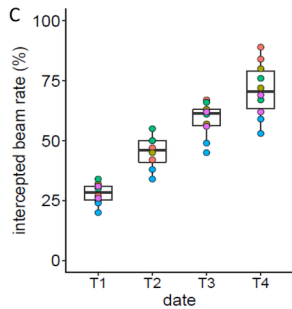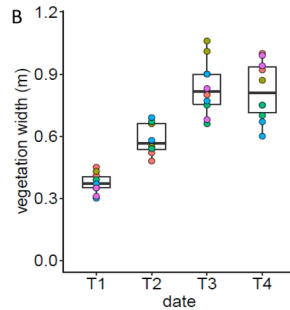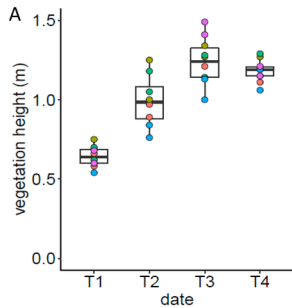
730

731   Figure 3. Relationship between the median deposition observed in 2016 and the median deposition in

732   2016 predicted from of univariate models for prediction of median deposition calibrated in 2017 on

733   the Collection, Faysse, Franquet and Petit Verdot blocks over the entire growing season (T1 red

734   square, T2 green triangle, T3 blue dot and T4 purple cross), coefficient of determination (R^2) of 0.79,

735   normalised root mean square error of prediction (nRMSEp) of 30% and bias of + 2.0%. The black

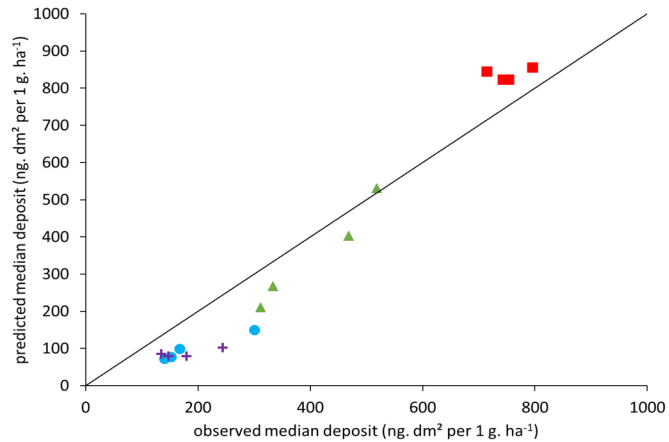736   curve represents a 1:1 linear curve.

737

738   Figure 4. a: Relationship between the median deposition observed in 2016 and the median deposition

739   predicted from multivariate models for prediction of median deposition calibrated in 2017 (T1 red

740   square, T2 green triangle, T3 blue dot and T4 purple cross), R^2 = 0.94, nRMSE = 13% and bias = -

741   2.1%. The black curve represents a 1:1 linear fit.
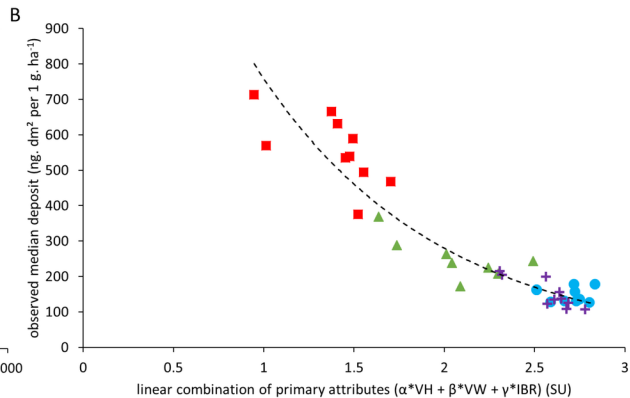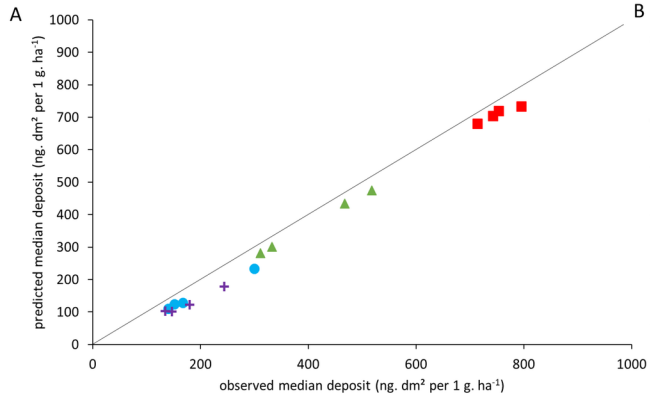
742   b: Evolution of D5 median spray deposits as a linear combination of primary canopy attributes

743   measured over the entire field and growing season (T1 red square, T2 green triangle, T3 blue dot and

744   T4 purple cross) in 2017. The dotted black curve represents the multivariate model for prediction of

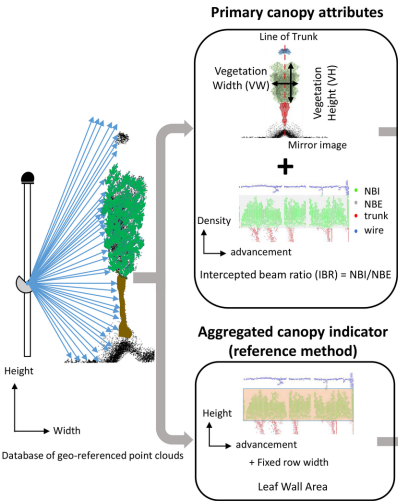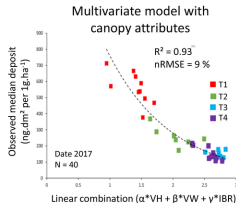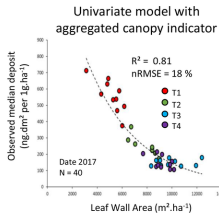745   median deposition (see D5 in Table 6 for parameters and statistics).

746

A

B

Primary canopy attributes

Line of Trunk

Vegetation Width (VW)

Vegetation Height (VH)

Mirror image

+

Density

advancement

NBI
NBE
trunk
wire

Intercepted beam ratio (IBR) = NBI/NBE

Aggregated canopy indicator (reference method)

Height

advancement

+ Fixed row width

Leaf Wall Area

Calibration step

Multivariate model with canopy attributes

$R^2 = 0.93$
nRMSE = 9 %

T1
T2
T3
T4

Date 2017
N = 40

Observed median deposit (ng.dm² per 1g.ha⁻¹)

Linear combination ($\alpha*VH + \beta*VW + \gamma*IBR$)

T1 = early season, T2 = early-mid season,
T3 = mid season, T4 = mid-late season

Univariate model with aggregated canopy indicator

$R^2 = 0.81$
nRMSE = 18 %

T1
T2
T3
T4

Date 2017
N = 40

Observed median deposit (ng.dm² per 1g.ha⁻¹)

Leaf Wall Area (m².ha⁻¹)

Spray deposition model quality (Validation data set)

Date 2016
N = 16

Multivariate model of decile depositions

Increasing model quality
Decreasing model uncertainty

Multivariate model of median deposition

Univariate model of median deposition

LiDAR generates local canopy dimensions. 1° canopy dimensions are better predictors than the current reference aggregated indicator and, modelling spray deposition distributions instead of the median improved deposition prediction models.

Height

Width

Database of geo-referenced point clouds